Plant Physiol. (1990) 93, 271–280
0032-0889/90/93/0271/10/$01.00/0

Received for publication September 20, 1989
and in revised form December 16, 1989

Measurement of Net Fluxes of Ammonium and Nitrate at the Surface of Barley Roots Using Ion-Selective Microelectrodes[1]

Gordon H. Henriksen*, Arnold J. Bloom, and Roger M. Spanswick

Section of Plant Biology, Division of Biological Sciences, Cornell University, Ithaca, New York 14853 (G.H.H., R.M.S.); *Department of Vegetable Crops, University of California, Davis, California 95616* (A.J.B.)

ABSTRACT

Neutral carrier-based liquid membrane ion-selective microelectrodes for NH_4^+ and NO_3^- were developed and used to investigate inorganic nitrogen acquisition in two varieties of barley, *Hordeum vulgare* L. cv Olli and *H. vulgare* L. cv Prato, originating in cold and warm climates, respectively. In the present paper, the methods used in the fabrication of ammonium- and nitrate-selective microelectrodes are described, and their application in the study of inorganic nitrogen uptake is demonstrated. Net ionic fluxes of NH_4^+ and NO_3^- were measured in the unstirred layer of solution immediately external to the root surface. The preference for the uptake of a particular ionic form was examined by measuring the net flux of the predominant form of inorganic nitrogen, with and without the alternative ion in solution. Net flux of NH_4^+ into the cold-adapted variety remained unchanged when equimolar concentrations (200 micromolar) of NH_4^+ and NO_3^- were present. Similarly, net flux of NO_3^- into the warm-adapted variety was not affected when NH_4^+ was also present in solution. The high temporal and spatial resolution afforded by ammonium- and nitrate-selective microelectrodes permits a detailed examination of inorganic nitrogen acquisition and its component ionic interactions.

Ammonium and nitrate are absorbed in greater amounts than any other ion present in the soil solution. The predominant form of inorganic nitrogen in a given soil depends largely on soil temperature, as the process of nitrification is more strongly inhibited by low temperature than ammonification (9). Therefore, plant varieties indigenous to warm or cold climates may be expected to adapt their mineral acquisition mechanisms to reflect the composition of their native soil solution.

To date, studies of inorganic nitrogen acquisition have relied primarily on measurements of the depletion of these two ions from solutions containing the root systems of intact plants or excised root segments. This approach integrates uptake over the entire root system for the duration of exposure to the test solution. Alternatively, ion uptake may be studied with a high degree of spatial and temporal resolution using ion-selective microelectrodes to measure ion activity gradients in the unstirred layer of solution immediately external to the root surface (11, 19). Newman *et al.* (19) have used this technique in conjunction with microelectrodes selective for K^+ and H^+ to investigate proposed mechanisms of K^+ uptake.

Here, we report on the fabrication and characteristics of neutral carrier-based ion-selective microelectrodes specific for NH_4^+ and NO_3^-, and demonstrate their use by investigating the preference of warm- and cold-adapted barley varieties for the form of inorganic nitrogen predominant in their native soils.

MATERIALS AND METHODS

Fabrication of Microelectrodes

Variables that influence the performance of a neutral carrier-based liquid membrane ion-selective microelectrode include: (a) type of glass, (b) tip diameter, (c) type and concentration of silane used to render the tip of the microelectrode hydrophobic, as well as the silane solvent and application method employed, (d) type of LIX[2] or solvent used to solubilize the neutral carrier, (e) length of the LIX column, (f) ionic strength and composition of the solution used to backfill the microelectrode, and (g) preconditioning of the microelectrode (1, 4, 26).

Borosilicate capillary blanks 10 cm long and 2 mm o.d. with an internal filament (World Precision Instruments, New Haven, CT, No. 1B200F-4) were pulled using a David Kopf model 700C vertical pipette puller. The silanization method used in the fabrication of these microelectrodes was that described by Borrelli *et al.* (4), in which a 2 to 5 mm column of 2 to 5% (v/v) tri-*N*-butylchlorosilane (Fluka, No. 90796) in carbon tetrachloride was injected into the tip of the micropipet. The micropipet was then placed on the surface of a hot plate (Corning, PC-35) for a period of 5 min. The temperature of the hot plate was adjusted such that a stainless steel-jacketed chromel-alumel thermocouple (Omega, KHSS-116G) connected to a digital multimeter (Beckman, HD110T) read 480°C when lying flat on the hot plate surface.

Because the microelectrodes would not be used intracellularly, the silanized micropipet tips were broken back to reduce the impedance. Using the method of controlled tip breakage

[1] Supported in part by National Science Foundation (N.S.F.) grant DMB 87-16363 (R. M. S.), N.S.F. grant DMB 88-06585 (A. J. B.), U. S. Department of Agriculture grant 88-37264-3857 (A. J. B.), and funds provided by the Hatch Program (R. M. S.).

[2] Abbreviations: LIX, liquid ion-exchange resin; PVC, poly(vinylchloride); THF, tetrahydrofuran; emf, electromotive force; FPM, fixed primary ion method; FIM, fixed interference method.

described by Tripathi *et al.* (27), one edge of a 10-cm-square piece of glassine-coated weighing paper was held down and the free end was allowed to hang over the edge of the bench. The tip of the micropipet was then slowly brushed across the surface of the paper. In this way, micropipets originally with tip diameters less than 1 μm could be broken back to 1 to 3 μm diameters in a fairly reproducible manner.

Micropipets were then back-filled with either 0.5 M NH_4Cl or 0.5 M KNO_3 and 0.1 M KCl for ammonium- and nitrate-selective microelectrodes, respectively. The micropipet tips were viewed under a compound microscope during this procedure. Once the back-filling solution had advanced to the tip, a syringe was connected to the back of the micropipet via a length of tygon tubing. At this point the appropriate LIX was front filled according to the method of Rink and Tsien (21). The tip was advanced into a drop of LIX at the end of a capillary tube and suction applied until a resin column 200 to 800 μm long was achieved. Microelectrodes were subsequently stored tip down for 6 to 12 h in a solution similar to the back-filling solution, as a preconditioning treatment before use.

The ammonium-selective ion exchange resin was prepared using 10% (w/w) of the macrotetralyde antibiotic nonactin (Fluka, No. 74155), 1% potassium tetrakis(4-chlorophenyl)borate (Fluka, No. 60591), and 2.5% PVC (Fluka, No. 81392), suspended in 86.5% dibutyl sebacate (Fluka, No. 84838). The mixture was diluted with 1 to 3 times its weight of tetrahydrofuran (Fluka, No. 87369) to solubilize the PVC. During the preconditioning period some of the THF diffuses out of the LIX and into the aqueous solution on either side of the liquid membrane, causing the resin column to shrink and become more viscous.

Nitrate-selective microelectrodes were fabricated using an ion exchange resin consisting of tris(substituted 1,10-phenanthroline) nickel(II) nitrate in *p*-nitrocymene (2), marketed by Orion (catalog No. 920702) for use in nitrate macroelectrodes.

Electronics

Ion-selective microelectrodes were inserted into a microelectrode holder (World Precisions Instruments, Inc., MEH-2S) and connected to the preamplifier of one channel of a high input impedance (10^{12} Ω) differential electrometer (World Precision Instruments, Inc., F-223). A double-junction reference electrode (Fisher No. 13-639-273) was connected to the preamplifier of the second channel. To minimize leakage of interfering ions into the test solutions, the outer body of the reference electrode was filled with 0.4 mM $MgSO_4$, to which was added a nonionic hydroxyethylcellulose thickening agent, Natrosol 250 (Aqualon Co., Wilmington, DE) at 6 g L^{-1}. The inner body was filled with 2.0 M KCl saturated with AgCl, and made more viscous with the addition of Natrosol at 10 g L^{-1}.

Calibration of Microelectrodes

Microelectrode calibrations were conducted by adding increasing amounts of the ion of interest to solutions previously adjusted to an ionic strength of 4.0 mM with $MgSO_4$. Using a dissociation constant of $K_D = 6.25 \times 10^{-3}$ (18), at a temperature of 20°C and 1 atm pressure, a 1.0 mM solution of $MgSO_4$ will be roughly 87% dissociated into Mg^{2+} and SO_4^{2-} ions (17, 25). The solutions were kept at a constant temperature of 20°C in a jacketed beaker connected to a circulating temperature-controlled water bath. Solutions were stirred constantly with a magnetic flea propelled by a turbine-driven magnetic stirrer (Thomas Scientific, No. 8612-B50).

Typically, microelectrodes were made in groups of eight, and the best selected from the group for experimental use. Selection was based primarily on three factors: slope (mV decade^{-1}), drift (mV min^{-1}), and response time. A preliminary test consisted of measuring the microelectrode response in a solution in which the concentration was increased from 10 to 100 and finally to 1000 μM by the addition of aliquots of concentrated solutions of the ion of interest. Once a microelectrode was selected, it was calibrated again between 1 and 1000 μM in the following sequence: 1, 2, 5, 10, 20, 50, 100, 200, 500, and 1000 μM.

The selectivity of the microelectrode against potentially interfering ions was determined by the fixed interference method (1, 8), in which a known amount of interfering ion was added to the calibration solution and the calibration performed as outlined above. The potentiometric selectivity factor (K_{ij}^{Pot}) was determined from the Nicolsky-Eisenman equation (1, 6)

$$K_{ij}^{Pot} = (a_i/a_j^{z_i/z_j}) \cdot 10^{z_i F(E_j - E_i)/2.303RT} \quad (1)$$

where i is the ion of interest, j is the interfering ion, E_i and E_j are the component potentials due to the ion of interest and the interfering ion respectively, z_i and z_j are the valence of the ion of interest and interfering ion respectively, a_i and a_j are the activities of the ions in solution, T is absolute temperature, R is the universal gas constant, and F is the Faraday. When E_i is equal to E_j, Equation 1 reduces to

$$K_{ij}^{Pot} = a_i/a_j^{z_i/z_j} \quad (2)$$

In the case of dilute solutions, ion concentrations may be substituted for ion activities (1). This is fortunate in that ion-selective electrodes measure activities while solutions are generally mixed according to concentration. The concentration of the ion of interest (C_i, virtually equivalent to its activity, a_i) at which E_i equals E_j is determined by extending the linear portions of the calibration curve to their point of intersection and reading the value of log C_i from the abscissa. The activity (concentration) of the interfering ion (a_j) is known and held constant in the fixed interference method.

Microelectrode response in the presence of interfering ions is dependent on the particular conditions in the test solution, including ionic strength, pH, and the ionic composition of the solution. Consequently, values of K_{ij}^{Pot} are only meaningful when the solution characteristics are specified, and are best used as rough estimates of the degree of interference rather than as mathematical correction factors.

Barley Culture

Seeds of two barley cultivars, *Hordeum vulgare* L. cv Olli and *H. vulgare* L. cv Prato, were germinated in the dark at

28°C on paper moistened with a solution of 200 μM $CaSO_4$. After 24 h, germinated seeds were suspended above light-tight, 1.5-L containers filled with 200 μM $CaSO_4$ into which air was bubbled, and placed in a growth chamber receiving light at a PPFD of 300 μmol m^{-2} s^{-1} for a 16 h photoperiod. Day and night temperatures were 18 and 15°C, respectively.

Net flux experiments were performed using seedlings 6 to 7 d from the start of germination in the case of Olli, or 4 to 5 d with Prato, as the seedlings had similar root and shoot lengths at these times.

In preparation for nitrate or ammonium flux experiments, several plants were transferred from aerated 200 μM $CaSO_4$ to aerated solutions consisting of 100 μM $Ca(NO_3)_2$ plus 100 μM $CaSO_4$ at least 12 h before the experiment. This was to ensure that the nitrate transport and reduction systems would be fully induced by the start of the experiment (10, 15).

Flux Measurements

Microelectrodes used in plant experiments were calibrated between 50 and 1000 μM, in solutions containing Ca^{2+} at 200 μM, and adjusted to an ionic strength of 4.4 mM with $MgSO_4$. To determine unknown ion activities in the unstirred layer of solution, a linear regression was performed on the five data points from the calibration and the resulting equation used to convert emf measurements to ion concentrations.

The experimental cuvette (Fig. 1) consisted of a 2.5-cm-thick stainless steel plate (9 cm by 18 cm) into which was cut a 4.5 cm by 14 cm chamber open on both sides. A piece of glass was fitted on the bottom side. The exposed steel surface on the bottom was coated with teflon. The stainless steel plate was drilled to allow a solution of polyethyleneglycol to circulate through the interior of the plate. The cuvette was attached to a micromanipulator (Sobotka, Farmingdale, NY) and situated on the teflon-covered stage of a Bausch and Lomb PhotoZoom inverted microscope. A motor-driven micromanipulator (Märzhäuser, DC-3K) was used to position the tip of the ion-selective microelectrode at the desired radial distances from the root surface.

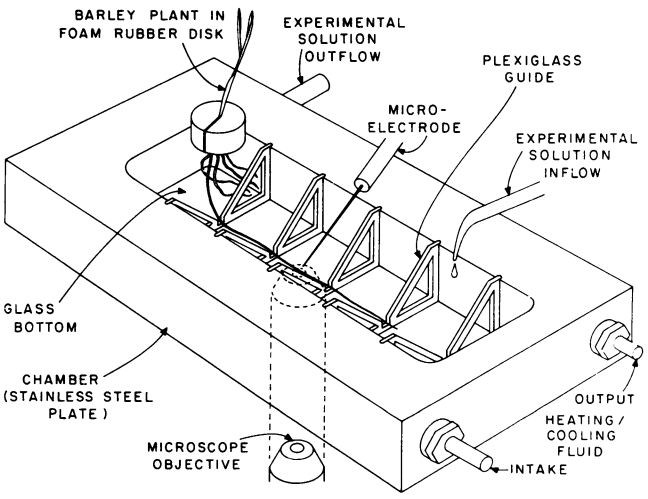

Figure 1. Stainless steel experimental cuvette. Cooling/heating solution flows through the cuvette interior and influences the experimental solution temperature through conduction. Experimental solutions flow into the chamber at one end and out at the other end. The cuvette is positioned on the stage of an inverted microscope and the barley root and microelectrode tip are viewed from below.

Root diameter and root axial location were measured using a calibrated eyepiece reticle at 40× magnification. The radial distance of the microelectrode tip from the root surface was determined at 100× using the same eyepiece reticle. Illumination of the root and microelectrode tip was supplied solely by room lighting; the microscope light remained off during the course of the experiment to avoid heating the solution in the cuvette and illuminating the root with strong light. The cuvette volume was 130 mL. Using solutions buffered at pH 4 and 8, the time required to flush the cuvette volume thoroughly was determined to be 6 min.

The solution delivery system included a loop whereby aerated solution could be cycled through the cuvette. This feature enabled us to insert a seedling in the chamber several hours before an experiment and thus allow sufficient time for recovery from movement and handling. This ensured that transport functions dependent upon a normal membrane potential would be operating. The cycled solution consisted of 100 μM $Ca(NO_3)_2$ and 100 μM $CaSO_4$.

All experimental solutions contained both the ion of interest and Ca^{2+} at 200 μM and were adjusted to an ionic strength of 4.4 mM using $MgSO_4$. In NH_4^+ net flux experiments, NH_4^+ was supplied as either $(NH_4)_2SO_4$ or NH_4NO_3. In NO_3^- net flux experiments, NO_3^- was supplied as either $Ca(NO_3)_2$ or NH_4NO_3.

At the start of an experiment, the first test solution was allowed to flow into the cuvette for 8 min. Because preliminary experiments showed that the diffusion profile becomes established within a few minutes of the cessation of solution inflow, measurements were begun within 10 min. The first potential reading was taken with the ion-selective microelectrode in the bulk solution (at least 5.0 mm from the root surface), then readings were taken at 100, 50, 25, 50, and 100 μm from the root surface, and finally again in the bulk solution (Fig. 2). Two to 3 min were allowed at each radial distance for a stable reading to be established. Following the conclusion of the first cycle of seven potential measurements,

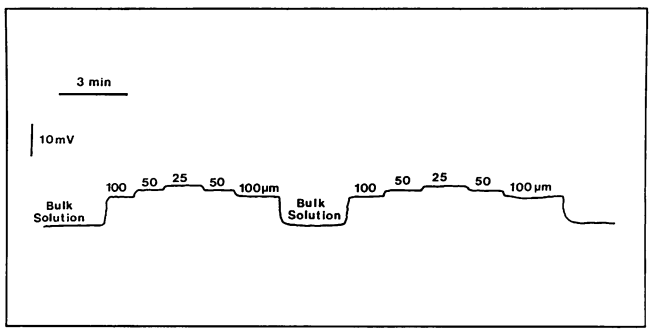

Figure 2. Typical stripchart recorder tracing of two cycles of net flux measurements. Each cycle (seven potential measurements) takes 10 to 15 min and produces two net flux values. Four cycles are completed before the experimental solution is changed. Response time of the microelectrode after positioning is less than 10 s.

the cycle was repeated three more times, then new solution was allowed to flow into the chamber and the entire process repeated for the new test solution. Each experiment involved six changes of solution. In control experiments, all six changes of solution were of the same composition. Alternatively, when net flux of NH_4^+ or NO_3^- was being tested in the presence of NO_3^- or NH_4^+, respectively, only the third and fourth solutions contained equimolar concentrations (200 μM) of both ions. The first, second, fifth, and sixth solutions were identical, consisting of the ion of interest; NH_4^+ in the case of Olli experiments, and NO_3^- in Prato experiments. At the conclusion of an experiment, the microelectrode was recalibrated between 50 and 1000 μM.

RESULTS AND DISCUSSION

Microelectrode Characteristics

In evaluating the performance and applicability of NH_4^+ and NO_3^- ion-selective microelectrodes, we investigated several characteristics: (a) limit of detection, (b) slope (mV decade^{-1}) within the anticipated concentration range, (c) amount of drift (mV min^{-1}), (d) practical response time of the electrode, (e) influence of pH, (f) effect of ionic strength, (g) influence of temperature, and (h) selectivity of the electrode against potentially interfering ions (8).

The limit of detection was determined in the course of constructing a calibration curve. The two linear portions of the curve were extended to their point of intersection and the concentration of the ion at this point, which corresponds to the limit of detection, was determined from the abscissa (Fig. 3; 8). In the case of NH_4^+-selective microelectrodes, the low end of the calibration curve had to be extended to include submicromolar ammonium concentrations. The limit of detection of a typical NH_4^+-selective microelectrode was found to be approximately 1 μM, while for NO_3^--selective microelectrodes it was 30 μM (Table I).

In the context of the present experimental system, the calculation of net fluxes from ion activity gradients in the unstirred layer of solution was facilitated by construction of

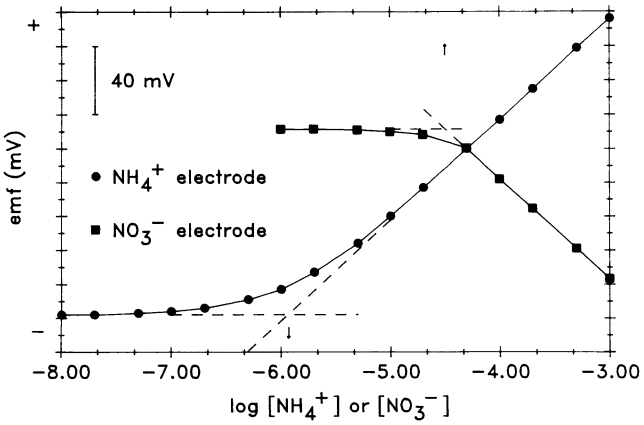

Figure 3. Typical calibration curves for NH_4^+ and NO_3^- microelectrodes. Ionic strength was adjusted to 4.4 mM with $MgSO_4$. The limit of detection was determined from the intersection of the linear portions of the curve.

Table I. *Characteristics of NH_4^+- and NO_3^--Selective Microelectrodes*

Electrode	Slope (100–1000 μM)	Limit of Detection	Drift
	mV/decade	*μM*	*mV/10 min*
NH_4^+	57.6 ± 1.1 (n = 78)	1	1.4 ± 0.9 (n = 6)
NO_3^-	57.3 ± 1.3 (n = 99)	32	0.1 ± 0.1 (n = 8)

a regression line with a high correlation coefficient. Any type of equation that accurately fits the calibration points may be used to determine unknown ionic activities from potential readings. Correction for electrode drift over the course of the experiment is made easier, however, if the calibration curve is linear in the range of the anticipated activities. Consequently, the lower limit of the useful working range must be raised to a point where the microelectrode response to changes in concentration is still linear. The slope of the microelectrode response in the anticipated experimental concentration range was determined from a regression line constructed using the calibration points between 50 and 1000 μM. The regression line fitted to the calibration points always had a correlation coefficient greater than 0.99. NH_4^+ and NO_3^- microelectrodes showed slopes of 57.6 and 57.3 mV decade $^{-1}$, respectively, in this concentration range (Table I).

At the conclusion of a calibration procedure, the microelectrode was left in solution ([NO_3^-] or [NH_4^+] = 1000 μM) and the drift measured over a period of 10 min. Typical NH_4^+ microelectrodes had an average drift of 1.4 mV over a 10 min period, while NO_3^- microelectrodes showed little drift, generally 0.1 mV in 10 min (Table I).

The practical response time of an ion-selective electrode is defined as the time required for the potential of the electrochemical cell to come to 90% of the final value from the moment at which the concentration of the ion of interest is changed (8). Due to the nature of the calibration protocol and the procedure for measuring net fluxes, the practical response time of NH_4^+- and NO_3^--selective microelectrodes was evaluated in a less rigorous manner.

In stirred calibration solutions, the time from the addition of a small aliquot of concentrated salt solution to the achievement of a stable reading is largely dependent on the rate of mixing. With the stirring speed held constant, several microelectrodes were calibrated in succession. Response time was then evaluated as the time required to achieve a stable reading after the addition of the last aliquot of solution. In general, roughly one minute was required, in the case of both NH_4^+ and NO_3^- microelectrodes.

During the course of an experiment, however, the solution in the cuvette was static and the microelectrode was moved through the diffusion profile. In this situation, the practical response time was a function of the time required to reposition the microelectrode in addition to the time for the electrode to respond to the change in concentration. The time required to move the tip of the microelectrode from the bulk solution to the 100 μm position was approximately 40 s. Only a second or two was needed to move the tip between positions within the unstirred layer. Figure 2 shows the response time of the

microelectrode to be only a few seconds in an unstirred solution.

Effect of pH

In experiments characterizing microelectrode response to changes in pH, the solution pH was monitored using a conventional combination pH electrode (Fisher, No. 13-620-252) and a digital pH meter (Orion, model 601A).

The effect of pH on electrode response can be considered in terms of the electrode's selectivity against H^+ or OH^-. In this context it was deemed more appropriate to use the fixed primary ion method (1) rather than the fixed interference method (8). Repeated calibrations in several solutions adjusted to different pH (FIM) would be more likely to introduce error and electrode variability than holding the ion concentration constant and varying the pH of the solution (FPM), through the addition of small aliquots of concentrated buffer solution. The concentration of the ion of interest was held at 200 μM and the initial ionic strength adjusted to 4.4 mM. The pH of the solution was varied using aliquots of 1.0 M Mes or 1.0 M Tris. Variation in the ionic strength of the solution over the course of the experiment was calculated to be less than 4.5%.

Ammonium-selective microelectrodes exhibited an increase in the emf in response to a ten-fold increase in $[H^+]$. In this respect, an increase in $[H^+]$ does produce a response similar to that expected from an increase in $[NH_4^+]$. However, the effect of increasing $[H^+]$ seems only significant between pH 6 and pH 8 (Fig. 4). This suggests that the effect is due rather to an increase in $[NH_4^+]$ resulting from a shift in the equilibrium between NH_4^+ and NH_3 (pK_a = 9.40 at 20°C). Were the offset due to an increase in $[H^+]$, one would expect an increase of the effect in the lower pH range.

Over the range of pH tested (pH 5.0–8.0), NO_3^- electrodes exhibited minimal sensitivity (Fig. 4). A 10-fold increase in $[OH^-]$ (or decrease in $[H^+]$) produced a change of +0.6 mV in the microelectrode response. This is interesting because it suggests that the influence of pH does not concern the selectivity of the NO_3^- microelectrode against OH^-. Were OH^- ions competing with NO_3^-, an increase in $[OH^-]$ would be expected to produce a negative offset, as is observed by increasing $[NO_3^-]$ (Fig. 3).

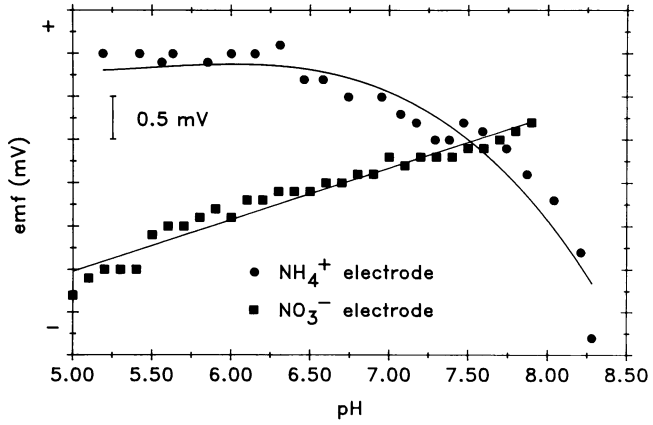

Figure 4. Effect of pH on microelectrode response. Curves are from typical NH_4^+ and NO_3^- microelectrodes. The concentration of the ion of interest was held constant at 200 μM, and ionic strength was initially adjusted to 4.4 mM using $MgSO_4$. pH was varied using small aliquots of either 1.0 M Mes or 1.0 M Tris.

Effect of Ionic Strength

The influence of ionic strength on the response of the microelectrode was determined by performing a series of calibrations on a single electrode. The ionic strength of the calibration solutions was adjusted to different values using $MgSO_4$. During the construction of a standard calibration curve, the ionic strength of the calibration solution will increase by approximately 37.5% due to the increase in the concentration of the ion of interest. We tested the influence of ionic strength on electrode response by increasing the ionic strength by 74.4%, from 4.3 to 5.4 to 6.5 to 7.5 mM.

Both NH_4^+ and NO_3^- microelectrodes showed virtually no sensitivity to these changes in ionic strength, within the range of concentrations in which the electrode response was linear (data not shown). Changes in ionic strength do influence, however, the electrode response near the limit of detection.

Effect of Temperature

Microelectrode response to temperature was determined by holding the concentration of the ion of interest constant at 200 μM and varying the temperature of the solution by inserting the calibration vessel in a temperature-controlled water bath. Test solution temperature was monitored continuously using a thermistor (Yellow Springs Instrument Co. Inc., model 404) and recorded, along with the microelectrode response, on a two-pen stripchart recorder (MFE Corp., Salem, NH, model 2125B). Solution temperatures were initially 30°C and were cooled to 10°C. The rate of cooling in the test solution was 0.2°C min^{-1}.

The potential of the electrode system, E, is given by

$$E = E_o + (2.303\ RT/z_iF)\cdot(\log a_i' - \log a_i'') \qquad (3)$$

where a_i' and a_i'' are the activities of the ion of interest in the external solution and the internal filling solution, respectively, and E_o is the sum of all the component potentials in the system with the exception of the emf across the LIX (1). If $a_i' < a_i''$, as is normally the case, an increase in temperature should produce a decrease in the emf of cation-selective electrodes (where z_i is positive) and an increase in the emf of anion-selective electrodes (where z_i is negative). Figure 5 illustrates this effect. The temperature coefficient for a typical NH_4^+-selective microelectrode is roughly 0.5 mV $°C^{-1}$, while the corresponding coefficient for a NO_3^--selective microelectrode is approximately 1.0 mV $°C^{-1}$. This is close to the theoretical value of 0.68 mV $°C^{-1}$, when a_i' is 200.00 μM and a_i'' is 0.5 M.

It is also important to note that the influence of temperature on the potential across the LIX increases as the value of a_i' diverges from the value of a_i''. Hence, the effect of temperature on E is most pronounced in dilute solutions and less noticeable as the solution concentration of the ion of interest

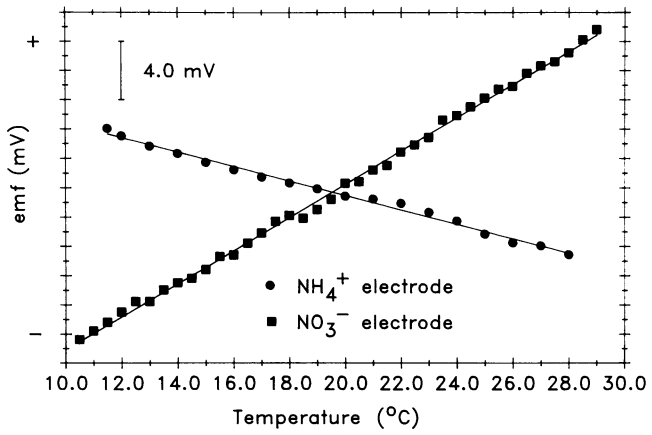

Figure 5. Effect of temperature on microelectrode response. Curves are from typical NH_4^+ and NO_3^- microelectrodes. The concentration of the ion of interest was held constant at 200 μM, and ionic strength was initially adjusted to 4.4 mM using $MgSO_4$. Temperature was reduced from 30 to 10°C at a rate of 0.2°C min^{-1}.

increases. When $a_i' = a_i''$, temperature will have no effect on the emf across the LIX.

Each of the component potentials in the electrode system will show a sensitivity to temperature, similar to that observed across the LIX, in keeping with the dictates of the Nernst equation (Eq. 3; 1). Therefore, changes in temperature outside the experimental solution must also be minimized, as they could influence the potentials at the Ag/AgCl electrodes, included in E_o.

Selectivity

In evaluating the selectivity of NH_4^+ microelectrodes, the cations tested as potentially interfering ions were K^+, Na^+, Ca^{2+}, and Mg^{2+}, due to their proximity in the Hofmeister series. In general, ions of similar valence pose a more severe problem as interfering ions. In this regard, 200 μM K^+ significantly influenced the electrode response (Fig. 6A). A potentiometric selectivity factor ($K^{Pot}_{NH_4K}$; Eq. 2) of about 0.1 was observed. Similarly, Na^+ exerted an interfering influence on NH_4^+ microelectrode response (Fig. 6B). In the presence of 3.13 mM Na^+, $K^{Pot}_{NH_4Na}$ was determined to be 0.002. While equimolar concentrations of Na^+ are of little concern, had our experimental solutions been adjusted to an ionic strength of 4.4 mM using Na_2SO_4, the resultant 10-fold excess of Na^+ would have caused unacceptable interference with the measurement of NH_4^+ activity gradients.

Both Ca^{2+} and Mg^{2+} exhibited little, if any, tendency to interfere with NH_4^+ microelectrode response. Calcium concentrations of 200 μM, similar to the level present in experimental solutions, had virtually no effect on the calibration of NH_4^+ microelectrodes (data not shown). Inasmuch as Mg^{2+} was present at high concentrations as an ionic strength adjuster, the selectivity of NH_4^+ electrodes against Mg^{2+} was tested with $[Mg^{2+}]$ at 1.0 and 1.8 mM. Again, no interference was observed (data not shown).

The monovalent anions tested for their ability to interfere with NO_3^- electrodes were Cl^- and HCO_3^- (Fig. 7). Although Cl^- was excluded from our experimental solutions, it is commonly present in biological solutions and must be considered as a potential interfering ion when using NO_3^- electrodes. Figure 7A reveals that Cl^- causes a slight amount of interference with NO_3^- microelectrodes, though the offset occurs primarily below the working range. With $[NO_3^-]$ at 100 μM, the offset due to a 30-fold excess of Cl^- was −6.5 mV. In the concentration range where the electrode response to NO_3^- is linear, a 10-fold increase in $[NO_3^-]$ causes an offset of −57.3 mV.

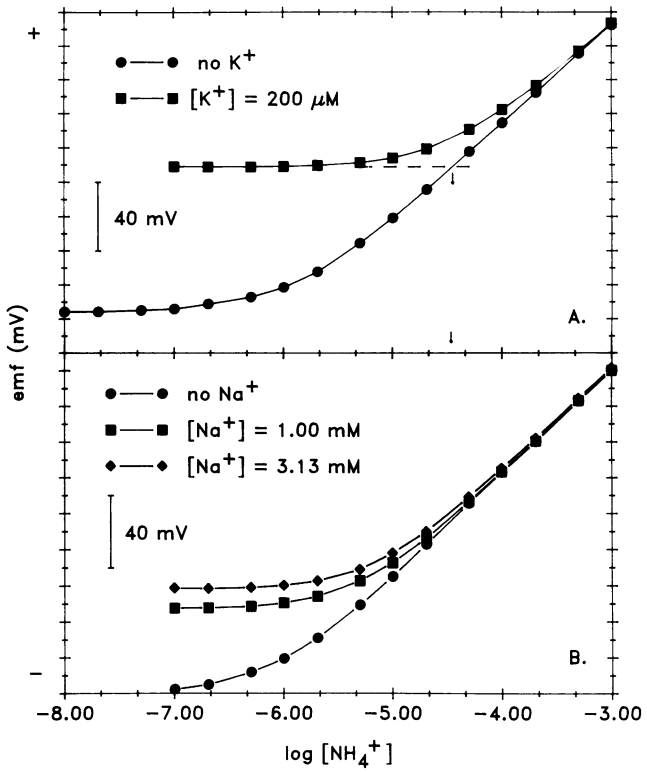

Figure 6. Selectivity of a typical NH_4^+ microelectrode against K^+ (A) and against Na^+ (B). Ionic strength was initially adjusted to 4.0 mM with $MgSO_4$. A standard calibration was performed with a fixed concentration of the interfering ion in solution. The potentiometric selectivity factor (K^{Pot}_{ij}) was determined from the intersection of the linear portions of the calibration curve (Eq. 2).

Interference due to HCO_3^- was tested by adding an aliquot of 0.1 M $NaHCO_3$ to give $[CO_2/HCO_3^-]$ of 200 μM (Fig. 7B). The pH of the unbuffered solution was 7.4, giving an actual $[HCO_3^-]$ of 183 μM. Again, in the linear range of the electrode response, the effect of a nearly equimolar amount of HCO_3^- was minimal. Similarly, interference due to SO_4^{2-} was tested and found to be negligible when solutions with a 10-fold and 20-fold excess of SO_4^{2-} were compared (data not shown).

Flux Measurements

Net fluxes were measured immediately upon insertion of the seedling into the cuvette or after plants had remained in the cuvette in aerated, circulating solution for at least 4 h to recover from any shock due to movement and handling.

Net flux experiments involved six changes of solution. Each solution remained in the experimental chamber for approxi-

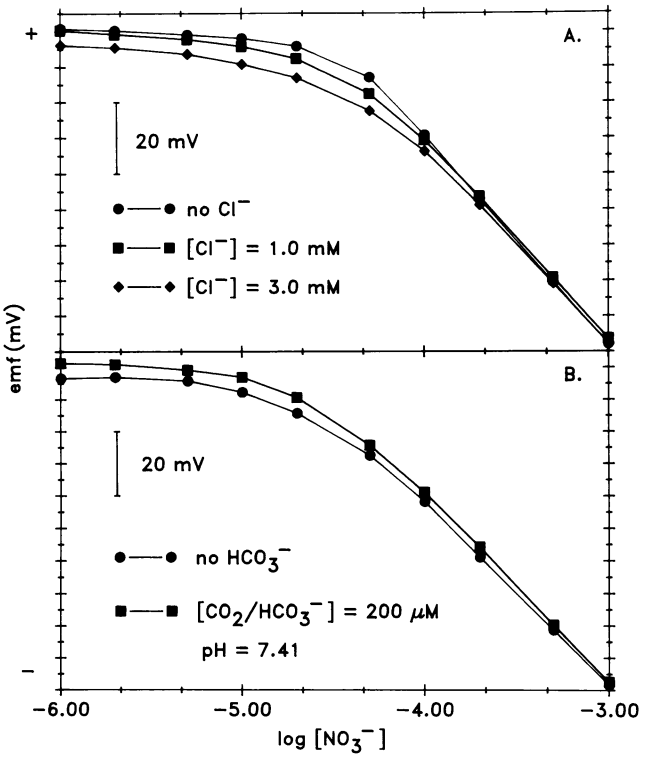

Figure 7. Selectivity of a typical NO_3^- microelectrode against Cl^- (A) and against HCO_3^- (B). Ionic strength was initially adjusted to 4.0 mM with $MgSO_4$. A standard calibration was performed with a fixed concentration of the interfering ion in solution. Initially, $[CO_2/HCO_3^-]$ was 200 μM through the addition of an aliquot of 0.1 M $NaHCO_3$. The pH throughout the calibration was 7.4, giving $[HCO_3^-]$ of 183 μM.

mately 1 h and, during this time, the series of seven potential measurements (in the bulk solution, at 100, 50, 25, 50, and 100 μm, and finally again in the bulk solution) was repeated four times. Each series of seven measurements produced two net flux values pairing the emf readings at radial distances of 100 and 50 μm, while moving the microelectrode toward the root surface, and at 50 and 100 μm moving the electrode away from the root (Fig. 2). Consequently, eight net flux values were determined during each of the six test solutions. Net flux values were calculated using the following equation

$$\phi = \frac{2\pi D_i^{*o} K(C_2 - C_1)}{A\rho \ln(r_2/r_1)} \quad (4)$$

where, ϕ is the net flux (μmol g fresh weight^{-1} h^{-1}), D_i^{*o} is the self-diffusion coefficient for the ion of interest (cm^2 s^{-1}), C_1 and C_2 are the concentrations of the ion of interest (nmol cm^{-3}) at radial distances r_1 and r_2 (μm) from the center of the root, A is the cross-sectional area of the root (cm^2), ρ is the density of the root tissue (g cm^{-3}), and K is a units conversion coefficient (11).

Self-diffusion coefficients for individual ions were calculated from limiting ionic conductivities (20) using the Nernst-Einstein relation

$$D_i^{*o} = \frac{RT\lambda_i^o}{|z_i|F^2} \quad (5)$$

where λ_i^o is the limiting ionic conductivity (referred to as "limiting ionic mobility" in earlier literature; 20) of the ion of interest (Ω^{-1} cm^2) and the other terms have their usual meaning (12, 22).

The limiting ionic conductivity values must be corrected for temperatures other than 25°C, using the empirical quadratic equation

$$\lambda^o = \lambda^o_{(25°C)} + a(T - 25) + b(T - 25)^2 + c(T - 25)^3. \quad (6)$$

Equation 6 is valid for values of T between 5 and 55°C. The constants a, b, and c are specific for each ion (20). In the absence of constants for NH_4^+ and NO_3^-, we substituted the constants for K^+ and Cl^- to correct the values of the limiting ionic conductivities given for 25°C to values appropriate for experiments conducted at 20°C. A comparison of the constants given for several cations and anions revealed little difference between neighbors in the Hofmeister series. The self-diffusion coefficients for NH_4^+ and NO_3^- at 20°C were calculated to be 1.74×10^{-5} and 1.67×10^{-5} cm^2 s^{-1}, respectively.

As indicated above, microelectrodes were calibrated immediately before and after the experiment. We observed two cases in comparing calibration curves constructed roughly six hours apart; (a) either the curves overlapped, indicating no change in electrode response over the course of the experiment, or (b) the curves were uniformly offset, the slope remaining unchanged while the intercept of the regression line through the points shifted.

Each time the microelectrode was moved into the bulk solution, corrections for electrode drift were made by recalculating the regression line intercept, based on the assumption that the background concentration of the ion of interest remained constant (200 μM) during the hour between solution changes.

Figure 8 demonstrates the effect of NO_3^- on NH_4^+ net flux in Olli barley. Three seedlings were used as controls (Fig. 8A) and were exposed to the same solution composition during each of the six solutions changes. This provided a test of whether net flux changed over the course of the 6 h experiment due to factors other than the presence of the alternate ion. Figure 8B shows the effect of an equimolar concentration of NO_3^- (during the third and fourth solution changes) on NH_4^+ net flux in three Olli barley seedlings. No change of a physiologically significant magnitude was observed in the net flux of NH_4^+ when Olli barley seedlings were offered NO_3^- in addition to NH_4^+.

Similarly, Figure 9 demonstrates the effect of NH_4^+ on NO_3^- net flux in Prato barley. Again, three seedlings were used as controls (Fig. 9A) and were exposed to the same solution composition during each of the six solution changes. Figure 9B shows the effect of an equimolar concentration of NH_4^+ (during the third and fourth solution changes) on NO_3^- net flux in three Prato seedlings. Net flux of NO_3^- remained relatively unchanged when Prato barley seedlings were supplied both NO_3^- and NH_4^+ at 200 μM. This is in contrast to the reports in the literature of significant reductions in NO_3^- net flux in the presence of NH_4^+ (5, 7, 13).

The limitations of both the technique and the microelectrodes themselves must be understood before any meaningful conclusions can be drawn from experiments of this type.

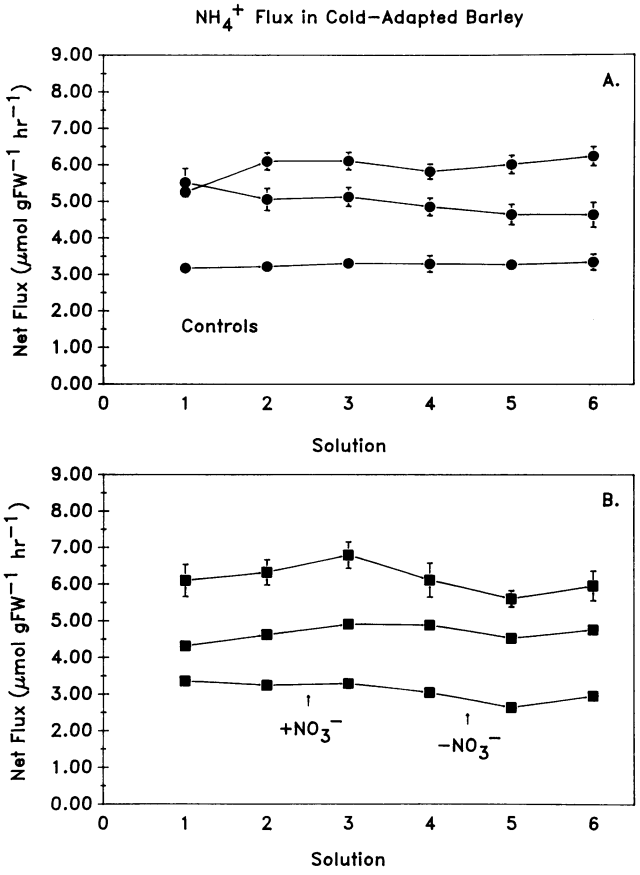

Figure 8. NH_4^+ net flux in Olli barley. Results of six separate experiments, each involving one Olli barley seedling. Each experiment involved six changes of solution. Data points are means ± SE of eight flux measurements in each solution. In control experiments (Fig. 8A) all six solutions were identical: 100 μM $(NH_4)_2SO_4$ and 200 μM $CaSO_4$, adjusted to an ionic strength of 4.4 mM with $MgSO_4$. In experiments testing the effect of NO_3^- on NH_4^+ net flux (Fig. 8B), solutions 3 and 4 consisted of 200 μM NH_4NO_3 and 200 μM $CaSO_4$, adjusted to an ionic strength of 4.4 mM with $MgSO_4$. Plants remained in each solution for approximately 1 h.

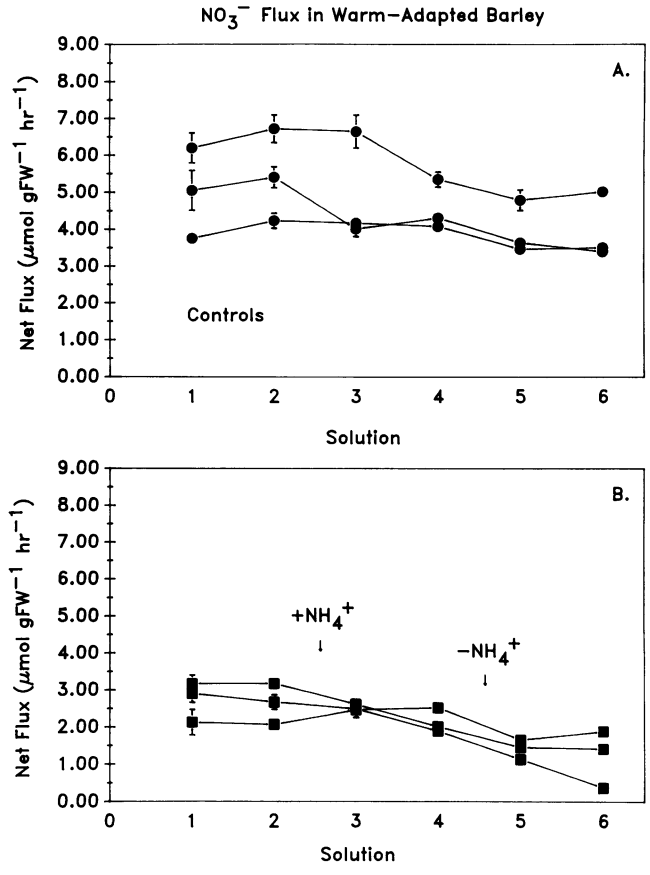

Figure 9. NO_3^- net flux in Prato barley. Results of six separate experiments, each involving one Prato barley seedling. Each experiment involved six changes of solution. Data points are means ± SE of eight flux measurements in each solution. In control experiments (A), all six solutions were identical: 100 μM $Ca(NO_3)_2$ and 100 μM $CaSO_4$, adjusted to an ionic strength of 4.4 mM with $MgSO_4$. In experiments testing the effect of NH_4^+ on NO_3^- net flux (B), solutions 3 and 4 consisted of 200 μM NH_4NO_3 and 200 μM $CaSO_4$, adjusted to an ionic strength of 4.4 mM with $MgSO_4$. Plants remained in each solution for approximately 1 h.

First, the microelectrodes are limited in their sensitivity to their respective ions. The construction of a calibration curve with closely spaced points permits their use to their limit of sensitivity, 1 μM for NH_4^+ microelectrodes, and 30 μM for NO_3^- microelectrodes. When linear regression equations are used to calculate unknown ion concentrations, however, the practical lower limit must be raised as the electrode response is not linear near the limit of detection. Concentrations used to generate the calibration regression line should bracket the expected experimental range of concentrations.

Second, interfering ions must be considered in calibrating ion-selective microelectrodes. Sources of interfering ions, in addition to these deliberately introduced as elements of experimental injury, include leakage of filling solution from reference electrodes, salts used to adjust the ionic strength of solutions, and efflux of ions from the plant itself.

In the case of NH_4^+ microelectrodes, K^+ presents the greatest interference. Because K^+ is readily transported into the plant, its concentration in solution will be changing. Hence, use of a calibration curve constructed with a constant background of the interfering ion is inappropriate. The $[K^+]$ at the point of measurement of $[NH_4^+]$ must be determined using a K^+-selective microelectrode in tandem with the NH_4^+ microelectrode, and a series of calibration curves constructed to determine what portion of the NH_4^+ microelectrode emf is attributable to K^+.

Third, temperature, due to its effect on electrode response, must be strictly controlled. As suggested by the Nernst equation, (Eq. 3), temperature will affect electrode response on the order of 0.68 mV °C^{-1}. Clearly, offsets of this magnitude are unacceptable, as the technique of Newman *et al.* (19) requires emf readings accurate to ±0.1 mV, (a 0.1 mV error in determining the difference between the emf at r_1 and the emf at r_2 causes a 7% difference in the calculated net flux). While significant temperature differences would not be expected over the distance between consecutive emf readings, they

could occur over the course of an entire experiment, and are quite likely during solution changes.

In addition, examination of the terms in Equation 4 reveals two ways in which a change in solution temperature must be taken into account in calculating the correct value of the net flux (ϕ). There will be an error introduced into the determination of the concentrations, C_1 and C_2, due to an effect on the slope of the calibration curve for the ion-selective microelectrode. In addition, the value of the self-diffusion coefficient, D_i^{*o}, varies with temperature. Equation 5 shows temperature exerting an influence on the self-diffusion coefficient directly, through T, as well as via the limiting ionic conductivity (λ°_i), itself a function of temperature (Eq. 6; 20). We estimate that an error of 1°C in determining solution temperature will also produce a 7% error in the calculation of the actual net flux at 20°C.

Fourth, as the bulk solution concentration of the ion of interest changes due to uptake, a means of correcting the calibration regression line and distinguishing between electrode drift and ion depletion due to uptake becomes important. To a rough approximation, the assumption that the bulk solution concentration remains constant is acceptable when the cuvette volume is large and the seedling root system is small. That situation allows easy adjustment of the regression line intercept and corrects for any electrode drift during the course of the experiment. When such is not the case, the ion concentration of the bulk solution must be measured independently.

Fifth, most studies of ion uptake, using either radioactive labels or ion-selective macroelectrodes to make bulk solution depletion measurements, involve perturbations to the plant material either through handling and transference between solutions, or through root excision.

In a series of control experiments (Fig. 9A), plants that had been situated overnight in 200 μM NO_3^- were inserted into the cuvette and flux measurements begun within 10 min. Over the first 120 min, NO_3^- flux showed a steady increase, similar in nature to the accelerated uptake of NO_3^- attributed to the induction of the nitrate transport and reduction systems (10, 15). It is our opinion, therefore, that handling of seedlings immediately prior to an experiment introduces an element of variability that is best eliminated by allowing plants sufficient time for recovery following insertion into the cuvette. Only in this way is it possible to say that the plant response is due to the nature of the ambient solution and not to its history of movement.

Many reports have appeared in the literature concerning the influence of ammonium on nitrate uptake in barley (3, 5, 7, 13), maize (14, 16, 23), and tomato (24). Deane-Drummond and Glass (5) have suggested that the influence of ammonium on nitrate net uptake depends on the amount of nitrate previously available. Using $^{36}ClO_3^-$ as an analog for NO_3^-, nitrate influx from a solution of 100 μM NO_3^- was not affected by the presence of 100 to 500 μM NH_4^+ if the seedlings had been previously grown at that nitrate concentration. They observed a stimulation of NO_3^- efflux in the presence of NH_4^+ and suggested that inhibition of net NO_3^- uptake by NH_4^+ is regulated through its effect on NO_3^- efflux.

In subsequent experiments using $^{13}NO_3^-$, however, Glass *et al.* (7) were able to show that 500 μM NH_4^+ caused a 50% reduction in influx, and that NO_3^- influx across the plasmalemma of intact barley plants was independent of pretreatment levels of NO_3^-. Their uptake medium contained NO_3^- at concentrations of either 422 or 750 μM. In addition, they observed 500 μM Cl^- in the external solution to be without effect on $^{13}NO_3^-$ influx. This led to the recommendation that experiments using $^{36}ClO_3^-$ as an analog of NO_3^- be interpreted with caution.

Lee and Drew (13) have also investigated the inhibition of $^{13}NO_3^-$ influx by ammonium in barley, and found 500 μM NH_4^+ to inhibit NO_3^- influx significantly within 3 min of exposure. They used external NO_3^- concentrations of either 1, 2.5, 15, 25, or 150 μM. Return to original NO_3^- influx rates occurred within 3 min of removal of NH_4^+. Their study also suggests that the inhibition of NO_3^- net uptake occurs primarily through the inhibition of NO_3^- influx and not through a stimulation of NO_3^- efflux.

In their investigation of warm- and cold-adapted barley varieties using ion-selective macroelectrodes, Bloom and Finazzo (3) observed an initial decline in NO_3^- net uptake in the presence of NH_4^+ for both Prato and Olli barley, followed by a partial return to the original rate over 2 to 3 h. They used equimolar concentrations of NO_3^- and NH_4^+, in the range of 1 to 200 μM. Although studies making use of ion-selective electrodes measure net uptake, and thus cannot distinguish between effects on influx and efflux, the experimental system used in their study had the advantage of allowing several hours for recovery after the plant was moved into the experimental chamber.

Similarly, the technique in the present study allowed an extended period for recovery from movement and handling before the start of the experiment. In addition, the use of ion-selective microelectrodes provides much greater spatial resolution, measuring net ionic flux in the vicinity of a small group of cells, and not integrating ion uptake over the entire root system. The temporal resolution afforded by this technique is a function of the response time of the microelectrode (a few seconds) and the time required for an effect at the root surface to be propagated by diffusion to the point of measurement (also a few seconds).

In this study, a statistical difference was observed between the control and NH_4^+-treated Prato barley plants (determined by ANOVA, General Linear Model Procedure, SAS), although the magnitude of the difference cannot be considered physiologically significant. Our results suggest that barley varieties acclimated to an environment in which one ionic form of nitrogen predominates, continue to take up that form in spite of the availability of the alternative form. As in the Bloom and Finazzo study, equimolar concentrations of NH_4^+ and NO_3^- were used when testing the inhibition of NO_3^- net uptake by NH_4^+, as well as the influence of NO_3^- on NH_4^+ net uptake.

Our primary purpose in presenting these results was to describe the fabrication of NH_4^+- and NO_3^--selective microelectrodes and to demonstrate their applicability in the study of inorganic nitrogen acquisition using the technique of Newman *et al.* (19). More detailed examinations of inorganic

nitrogen uptake in warm- and cold-adapted barley varieties are in progress.

ACKNOWLEDGMENT

The authors wish to express their gratitude to Dr. Timothy C. Dorsey for his recommendations and assistance in the statistical analysis of the net flux data, and to Dr. Christopher D. Faraday for his helpful comments on the manuscript.

LITERATURE CITED

1. **Ammann D** (1986) Ion-Selective Microelectrodes: Principles, Design, and Application. Springer-Verlag, New York
2. **Bailey PL** (1976) Analysis with Ion-Selective Electrodes. Heyden & Son Ltd., New York
3. **Bloom A, Finazzo J** (1986) Influence of ammonium and chloride on potassium and nitrate absorption by barley roots depends on time of exposure and cultivar. Plant Physiol **81:** 67–69
4. **Borrelli M, Carlini W, Dewey W, Ransom B** (1985) A simple method for making ion-selective microelectrodes suitable for intracellular recording in vertebrate cells. J Neurosci Methods **15:** 141–154
5. **Deane-Drummond CE, Glass ADM** (1983) Short term studies of nitrate uptake into barley plants using ion-specific electrodes and $^{36}ClO_3^-$. II. Regulation of NO_3^- efflux by NH_4^+. Plant Physiol **73:** 105–110
6. **Eisenman G** (1967) Glass Electrodes for H^+ and Other Cations: Principles and Practice. Marcel Dekker Inc., New York
7. **Glass ADM, Thompson RG, Bordeleau L** (1985) Regulation of NO_3^- influx in barley. Plant Physiol **77:** 379–381
8. **Guilbault GG** (1979) Recommendations for publishing manuscripts on ion-selective electrodes. Ion-Selective Electrode Rev **1:** 139–143
9. **Haynes RJ, Goh KM** (1978) Ammonium and nitrate nutrition of plants. Biol Rev **53:** 465–510
10. **Jackson WA, Flesher D, Hageman RH** (1973) Nitrate uptake by dark-grown corn seedlings. Some characteristics of apparent induction. Plant Physiol **51:** 107–112
11. **Kochian LV, Newman IA, Lucas WJ** (1990) Ion transport in corn roots: localized stoichiometries for protons, potassium and chloride. Seventh Annual Workshop on Plant Membrane Transport, 24–29 August, Sydney, Australia (in press)
12. **Koryta J, Dvorak J** (1987) Principles of Electrochemistry. John Wiley & Sons Ltd., New York
13. **Lee RB, Drew MC** (1989) Rapid, reversible inhibition of nitrate influx in barley by ammonium. J Exp Bot **40:** 741–752
14. **MacKown CT, Jackson WA, Volk RJ** (1982) Restricted nitrate influx and reduction in corn seedlings exposed to ammonium. Plant Physiol **69:** 353–359
15. **MacKown CT, McClure PR** (1988) Development of accelerated net nitrate uptake. Effects of nitrate concentration and exposure time. Plant Physiol **87:** 162–166
16. **MacKown CT, Volk RJ, Jackson WA** (1982) Nitrate assimilation by decapitated corn root systems: effects of ammonium during induction. Plant Sci Lett **24:** 295–302
17. **Monk CB** (1961) Electrolytic Dissociation. Academic Press, New York
18. **Nair VSK, Nancollas GH** (1958) Thermodynamics of ion association. Part IV. Magnesium and zinc sulphates. J Chem Soc **4:** 3706–3710
19. **Newman IA, Kochian LV, Grusak M, Lucas WJ** (1987) Fluxes of H^+ and K^+ in corn roots: characterization and stoichiometries using ion-selective microelectrodes. Plant Physiol **84:** 1177–1184
20. **Parsons R** (1959) Handbook of Electrochemical Constants. Butterworths Scientific Publications, London
21. **Rink T, Tsien R** (1980) Calcium-selective micro-electrodes with bevelled, submicron tips containing poly(vinylchloride)-gelled neutral-ligand sensor. J Physiol **308:** 5P–6P
22. **Robinson RA, Stokes RH** (1959) Electrolyte Solutions, Ed 2. Butterworths Scientific Publications, London
23. **Rufty TW Jr, Jackson WA, Raper CD Jr** (1982) Inhibition of nitrate assimilation in roots in the presence of ammonium: The moderating influence of potassium. J Exp Bot **33:** 1122–1137
24. **Smart DR, Bloom AJ** (1988) Kinetics of ammonium and nitrate uptake among wild and cultivated tomatoes. Oecologia **76:** 336–340
25. **Smedley SI** (1980) The Interpretation of Ionic Conductivity in Liquids. Plenum Press, New York
26. **Thomas RC** (1978) Ion-Sensitive Intracellular Microelectrodes: How to Make and Use Them. Academic Press, New York
27. **Tripathi S, Morgunov N, Boulpaep E** (1985) Submicron tip breakage and silanization control improve ion-selective microelectrodes. Am J Physiol **249:** C514–C521